J. Plasma Physics (2009), *vol.* 75, *part* 4, *pp.* 475–493.
doi:10.1017/S0022377808007733 Printed in the United Kingdom

Multi-dimensional instability of dust-ion-acoustic solitary waves in a multi-ion dusty plasma

M. G. M. ANOWAR[1] and A. A. MAMUN[2]

[1] Department of Physics, National University, Gazipur-1704, Bangladesh (g.anowar@yahoo.com)

[2] Department of Physics, Jahangirnagar University, Savar, Dhaka-1342, Bangladesh

(Received 10 August 2008 and in revised form 23 October 2008, first published online 11 December 2008)

Abstract. The basic features of obliquely propagating dust-ion-acoustic (DIA) solitary waves, and their multi-dimensional instability in a magnetized multi-ion dusty plasma containing hot adiabatic inertia-less electrons, cold positive and negative ions, and negatively charged static dust have been theoretically investigated by the reductive perturbation method, and the small-k perturbation expansion technique. The combined effects of electron adiabaticity, external magnetic field (obliqueness), and negative ions, which are found to significantly modify the basic properties (speed, amplitude, width, and instability) of small but finite-amplitude DIA solitary waves, are explicitly examined. It is also found that the instability criterion and the growth rate are significantly modified by the external magnetic field, the propagation directions of both the nonlinear waves and their perturbation modes, and the presence of negative ions. The implications of our results in space and laboratory dusty plasmas are briefly discussed.

1. Introduction

Dust is ubiquitous in most space and astrophysical plasma systems, such as molecular clouds, protostellar disks, interstellar and circumstellar clouds, asteroid zones, planetary atmospheres, interstellar media, cometary tails, nebula, Earth's ionosphere, etc. (Geortz 1989; Mendis and Horanyi 1991; Mendis and Rosenberg 1994; Pieper and Goree 1996; Birk et al. 1996; Copp et al. 1997; Shukla et al. 1997, 1999; Rosenberg and Shukla 2002; Kourakis et al. 2005; Vranjes et al. 2005; Rosenberg and Merlino 2007). Dust particles are not neutral, but are charged either negatively or positively depending on the ambient plasma environments (Geortz 1989; Mendis and Rosenberg 1994; Verheest 2000; Shukla and Mamun 2002). Therefore, electrostatic and electromagnetic modes and associated instabilities in dusty magnetoplasmas have received a remarkable renewed interest because of their vital role in understanding the dynamics and fragmentation of molecular clouds, the star formation, the galactic structure and its evolution, the magnetic reconnection, the spoke formation of Saturn's rings, etc. (Horanyi and Mendis 1985, 1986; Geortz 1989; Northrop 1992; Mendis and Horanyi 1991; Montmerle 1991; Ciolek and Mouschovias 1993; Mendis and Rosenberg 1994; Nakano et al. 1996).

It was first theoretically shown (Shukla and Silin 1992) that due to the conservation of equilibrium charge density $n_{e0} + n_{d0} Z_d = n_{i0}$, and the strong inequality

$n_{e0} \ll n_{i0}$ (where n_{i0}, n_{e0}, and n_{d0} are the ion, electron, and dust number densities, respectively, Z_d is the number of electrons residing on the dust grain surface, and e is the magnitude of the electronic charge) a dusty plasma (with negatively charged static dust) supports low-frequency dust-ion-acoustic (DIA) waves with phase speed much smaller (larger) than the electron (ion) thermal speed. The dispersion relation of the linear DIA waves is (Shukla and Silin 1992) $\omega^2 = (n_{i0}/n_{e0})k^2C_i^2/(1+k^2\lambda_{De}^2)$, where $C_i = (k_BT_{e0}/m_i)^{1/2}$ is the ion-acoustic speed (with T_{e0} being the electron temperature at equilibrium and m_i being the ion mass, k_B being the Boltzmann constant) and $\lambda_{De} = (k_BT_{e0}/4\pi n_{e0}e^2)^{1/2}$ is the electron Debye radius. When a long wavelength limit (viz. $k\lambda_{De} \ll 1$) is considered, the dispersion relation for the DIA waves becomes $\omega = (n_{i0}/n_{e0})^{1/2}kC_i$. This form of spectrum is similar to the usual ion-acoustic wave spectrum for a plasma with $n_{i0} = n_{e0}$ and $T_{i0} \ll T_{e0}$ (where T_{i0} is the ion temperature at equilibrium). However, in dusty plasmas we usually have $n_{i0} \gg n_{e0}$ and $T_{i0} \simeq T_{e0}$. Therefore, a dusty plasma cannot support the usual ion-acoustic waves, but support the DIA waves of Shukla and Silin (1992). The DIA waves have also been experimentally observed (Barkan et al. 1996). The linear properties of the DIA waves in dusty plasmas are now well understood from both theoretical and experimental points of view (Shukla and Silin 1992; Barkan et al. 1996; Shukla and Rosenberg 1999; Shukla and Mamun 2002). The nonlinear features of the (DIA) waves have also received a great deal of interest when considering the understanding of the basic properties of localized electrostatic perturbations in space and laboratory dusty plasmas (Bharuthram and Shukla 1992; Barkan et al. 1996; Nakamura et al. 1999; Nakamura and Sharma 2001; Shukla and Mamun 2002, 2003; El-Labany and El-Shamy 2004. The DIA solitary waves (SWs) have also been investigated by several authors (Bharuthram and Shukla 1992; Mamun and Shukla 2002a,b, 2005; Rahman et al. 2007), but these works are valid only for an unmagnetized dusty plasma with cold ions and isothermal (Maxwellian) electrons. Recently, Mamun (2008) has investigated the basic properties of one-dimensional DIA SWs in an unmagnetized adiabatic dusty plasma, which contains non-inertial adiabatic electrons, inertial adiabatic ions, and negatively charged static dust. On the other hand, Sayed et al. (2008) have studied the DIA SWs in unmagnetized multi-ion dusty plasma containing inertialess isothermal electrons, cold inertial positive and negative ions, and negatively charged static dust. It is well known that the effects of the external magnetic field and obliqueness, which have not been considered in the earlier investigations (Bharuthram and Shukla 1992; Mamun and Shukla 2002a,b, 2005; Rahman et al. 2007; Mamun 2008; Sayed et al. 2008), drastically modify the basic properties of the ion-acoustic SWs (Shukla and Yu 1978; Lee and Kan 1981; Witt and Lotko 1983). Therefore, in our present work, we consider a magnetized multi-ion dusty plasma containing non-inertial hot adiabatic electrons, cold positive and negative ions, and negatively charged static dust, and study the properties of the obliquely propagating DIA SWs and their multi-dimensional instability in such a magnetized dusty plasma.

This paper is organized as follows. The basic equations governing the magnetized multi-ion dusty plasma system are given in Sec. 2. The Zakharov–Kuznetsov (ZK) equation is derived by employing a reductive perturbation method in Sec. 3. The stationary SW solution of the ZK equation and its basic features are studied in Sec. 4. The instability criterion is analyzed in Sec. 5. Finally, a brief discussion is presented in Sec. 6.

2. Governing equations

We consider a fully ionized collisionless magneto dusty plasma consisting of cold positive and negative ions, hot adiabatic inertia-less electrons, and negatively charged static dust in the presence of an external static magnetic field $\mathbf{B}_0 = B_0\hat{\mathbf{z}}$. The nonlinear dynamics of the DIA waves in this plasma system is described by

$$\frac{\partial N_{\rm i}}{\partial T} + \nabla \cdot (N_{\rm i}\mathbf{U}_{\rm i}) = 0, \tag{2.1}$$

$$\frac{\partial \mathbf{U}_{\rm i}}{\partial T} + (\mathbf{U}_{\rm i} \cdot \nabla)\mathbf{U}_{\rm i} = -\nabla\psi + \Omega_{\rm ci}\mathbf{U}_{\rm i} \times \hat{z}, \tag{2.2}$$

$$\frac{\partial N_{-\rm i}}{\partial T} + \nabla \cdot (N_{-\rm i}\mathbf{U}_{-\rm i}) = 0, \tag{2.3}$$

$$\frac{\partial \mathbf{U}_{-\rm i}}{\partial T} + (\mathbf{U}_{-\rm i} \cdot \nabla)\mathbf{U}_{-\rm i} = \sigma\nabla\psi - \sigma\Omega_{\rm ci}\mathbf{U}_{-\rm i} \times \hat{z}, \tag{2.4}$$

$$\frac{\partial N_{\rm e}}{\partial T} + \nabla \cdot (N_{\rm e}\mathbf{U}_{\rm e}) = 0, \tag{2.5}$$

$$0 = \nabla\psi - \Omega_{\rm ci}\mathbf{U}_{\rm e} \times \hat{z} - \frac{1}{N_{\rm e}}\nabla P_{\rm e}, \tag{2.6}$$

$$\frac{\partial P_{\rm e}}{\partial T} + \mathbf{U}_{\rm e} \cdot \nabla P_{\rm e} + \gamma_{\rm e}P_{\rm e}\nabla \cdot \mathbf{U}_{\rm e} = 0, \tag{2.7}$$

$$\nabla^2\psi = \mu N_{\rm e} - N_{\rm i} + \mu_- N_{-\rm i} - \mu_{\rm d}, \tag{2.8}$$

where $N_{\rm i}$, $N_{\rm e}$, $N_{-\rm i}$ are the positive ion, electron and negative ion number densities normalized by their equilibrium values $n_{\rm i0}$, $n_{\rm e0}$, $n_{-\rm i0}$, respectively, $\mathbf{U}_{\rm i}$, $\mathbf{U}_{\rm e}$, $\mathbf{U}_{-\rm i}$ are the positive ion, electron, negative ion fluid velocities, respectively, normalized by the ion-acoustic speed $C_{\rm i}$, ψ is the electrostatic wave potential normalized by $k_{\rm B}T_{\rm e0}/e$, $\mu = n_{\rm e0}/n_{\rm i0}$, $\mu_- = (Z_{-\rm i}n_{-\rm i0})/n_{\rm i0}$, $Z_{-\rm i}$ is the number of electrons residing on the negative ion, $\sigma = (Z_{-\rm i}m_{\rm i})/m_{-\rm i}$ with $m_{-\rm i}$ is the negative ion mass, and $\mu_{\rm d} = 1 - \mu - \mu_-$. $\gamma_{\rm e} = C_{\rm p}^{\rm e}/C_{\rm v}^{\rm e}$, where $C_{\rm p}^{\rm e}$ ($C_{\rm v}^{\rm e}$) is the specific heat of the electron fluid at constant pressure (volume). Also $\Omega_{\rm ci}$ is the ion cyclotron frequency normalized by the ion plasma frequency $\omega_{\rm pi} = (4\pi e^2 n_{\rm i0}/m_{\rm i})^{1/2}$, and $P_{\rm e}$ is the electron pressure normalized by $n_{\rm e0}k_{\rm B}T_{\rm e0}$. The time variable T is normalized by the ion plasma period $\omega_{\rm pi}^{-1}$, and the space variable is normalized by the Debye radius $\lambda_{\rm D} = (k_{\rm B}T_{\rm e0}/4\pi e^2 n_{\rm i0})^{1/2}$.

3. Derivation of ZK equation

We now follow the reductive perturbation technique and construct a weakly nonlinear theory for the electrostatic waves with a small but finite amplitude, which leads to a scaling of the independent variables through the stretched coordinates (Laedke and Spatschek 1982; Infeld 1985) $X = \epsilon^{1/2}x$, $Y = \epsilon^{1/2}y$, $Z = \epsilon^{1/2}(z - V_{\rm p}T)$, and $\tau = \epsilon^{3/2}T$, where ϵ is a small parameter measuring the weakness of the dispersion, $V_{\rm p}$ is the unknown wave phase speed (to be determined later). It may be noted here that X, Y, and Z are all normalized by the Debye radius ($\lambda_{\rm D}$), τ is normalized by the ion plasma period ($\omega_{\rm pi}^{-1}$), and $V_{\rm p}$ is normalized by the ion-acoustic speed ($C_{\rm i}$). We can now expand the perturbed quantities about their equilibrium values

https://doi.org/10.1017/S0022377808007733 Published online by Cambridge University Press

in powers of ϵ as (Laedke and Spatschek 1982, Infeld 1985)

$$3N_s = 1 + \epsilon N_s^{(1)} + \epsilon^2 N_s^{(2)} + \cdots, \quad U_{sz} = \epsilon U_{sz}^{(1)} + \epsilon^2 U_{sz}^{(2)} + \cdots, \tag{3.1}$$

$$U_{sx} = \epsilon^{3/2} U_{sx}^{(1)} + \epsilon^2 U_{sx}^{(2)} + \cdots, \quad U_{sy} = \epsilon^{3/2} U_{sy}^{(1)} + \epsilon^2 U_{sy}^{(2)} + \cdots, \tag{3.2}$$

$$P_{\rm e} = 1 + \epsilon P_{\rm e}^{(1)} + \epsilon^2 P_{\rm e}^{(2)} + \cdots, \quad \psi = \epsilon \psi^{(1)} + \epsilon^2 \psi^{(2)} + \cdots, \tag{3.3}$$

where $s = {\rm i}$ stands for positive ion, $s = -{\rm i}$ stands for negative ion, and $s = {\rm e}$ stands for electron species.

We now use the stretched coordinates and (3.1)–(3.3) in (2.1)–(2.8), and develop equations in various powers of ϵ. To the lowest order in ϵ, i.e., equating the coefficients of $\epsilon^{3/2}$ from the continuity, momentum, and pressure equations, one can obtain the first-order continuity equations, pressure equations, and x, y, and z components of the momentum equations, which in turn give

$$N_{\rm i}^{(1)} = \frac{1}{V_{\rm p}^2}\psi^{(1)}, \quad N_{-{\rm i}}^{(1)} = -\frac{\sigma}{V_{\rm p}^2}\psi^{(1)}, \quad N_{\rm e}^{(1)} = \frac{1}{\gamma_{\rm e}}\psi^{(1)}, \tag{3.4}$$

$$U_{{\rm i}x}^{(1)} = -\frac{1}{\Omega_{\rm ci}}\frac{\partial \psi^{(1)}}{\partial Y}, \quad U_{{\rm i}y}^{(1)} = \frac{1}{\Omega_{\rm ci}}\frac{\partial \psi^{(1)}}{\partial X}, \quad U_{{\rm i}z}^{(1)} = \frac{1}{V_{\rm p}}\psi^{(1)}, \tag{3.5}$$

$$U_{-{\rm i}x}^{(1)} = -\frac{1}{\Omega_{\rm ci}}\frac{\partial \psi^{(1)}}{\partial Y}, \quad U_{-{\rm i}y}^{(1)} = \frac{1}{\Omega_{\rm ci}}\frac{\partial \psi^{(1)}}{\partial X}, \quad U_{-{\rm i}z}^{(1)} = -\frac{\sigma}{V_{\rm p}}\psi^{(1)}, \tag{3.6}$$

$$U_{{\rm e}x}^{(1)} = U_{{\rm e}y}^{(1)} = 0, \quad U_{{\rm e}z}^{(1)} = \frac{1}{\gamma_{\rm e}} V_{\rm p}\psi^{(1)}, \quad P_{\rm e}^{(1)} = \psi^{(1)}. \tag{3.7}$$

Equating the coefficients of ϵ from Poisson's equation, we get

$$\mu N_{\rm e}^{(1)} = N_{\rm i}^{(1)} - \mu_- N_{-{\rm i}}^{(1)}. \tag{3.8}$$

Using (3.4) in (3.8), we get the linear dispersion relation

$$V_{\rm p} = \sqrt{\frac{\gamma_{\rm e}(1 + \mu_-\sigma)}{\mu}}. \tag{3.9}$$

The first two equations of (3.5) and (3.6) are also satisfied by the next higher (second) order continuity equations. Similarly, to the next higher order of ϵ, we obtain the second order x and y components of the momentum equations and Poisson's equation as

$$U_{{\rm i}x}^{(2)} = \frac{V_{\rm p}}{\Omega_{\rm ci}^2}\frac{\partial^2 \psi^{(1)}}{\partial Z \partial X}, \quad U_{{\rm i}y}^{(2)} = \frac{V_{\rm p}}{\Omega_{\rm ci}^2}\frac{\partial^2 \psi^{(1)}}{\partial Z \partial Y}, \tag{3.10}$$

$$U_{-{\rm i}x}^{(2)} = -\frac{V_{\rm p}}{\sigma\Omega_{\rm ci}^2}\frac{\partial^2 \psi^{(1)}}{\partial Z \partial X}, \quad U_{-{\rm i}y}^{(2)} = -\frac{V_{\rm p}}{\sigma\Omega_{\rm ci}^2}\frac{\partial^2 \psi^{(1)}}{\partial Z \partial Y}, \tag{3.11}$$

$$U_{{\rm e}x}^{(2)} = U_{{\rm e}y}^{(2)} = 0, \tag{3.12}$$

$$\left[\frac{\partial^2}{\partial X^2} + \frac{\partial^2}{\partial Y^2} + \frac{\partial^2}{\partial Z^2}\right]\psi^{(1)} = \mu N_{\rm e}^{(2)} - N_{\rm i}^{(2)} + \mu_- N_{-{\rm i}}^{(2)}. \tag{3.13}$$

https://doi.org/10.1017/S0022377808007733 Published online by Cambridge University Press

Following the same procedure one can obtain the next higher order continuity equations, pressure equations, and the z component of momentum equations as

$$\frac{\partial \psi^{(1)}}{\partial \tau} - V_{\rm p}^3 \frac{\partial N_{\rm i}^{(2)}}{\partial Z} + V_{\rm p}^2 \frac{\partial U_{{\rm i}z}^{(2)}}{\partial Z} + \frac{2}{V_{\rm p}} \psi^{(1)} \frac{\partial \psi^{(1)}}{\partial Z} + \frac{V_{\rm p}^3}{\Omega_{\rm ci}^2} \left[\frac{\partial^3 \psi^{(1)}}{\partial Z \partial X^2} + \frac{\partial^3 \psi^{(1)}}{\partial Z \partial Y^2} \right] = 0, \tag{3.14}$$

$$\frac{\partial \psi^{(1)}}{\partial \tau} - V_{\rm p}^2 \frac{\partial U_{{\rm i}z}^{(2)}}{\partial Z} + V_{\rm p} \frac{\partial \psi^{(2)}}{\partial Z} + \frac{1}{V_{\rm p}} \psi^{(1)} \frac{\partial \psi^{(1)}}{\partial Z} = 0, \tag{3.15}$$

$$\frac{\partial \psi^{(1)}}{\partial \tau} + \frac{V_{\rm p}^3}{\sigma} \frac{\partial N_{-{\rm i}}^{(2)}}{\partial Z} - \frac{V_{\rm p}^2}{\sigma} \frac{\partial U_{-{\rm i}z}^{(2)}}{\partial Z} - \frac{2\sigma}{V_{\rm p}} \psi^{(1)} \frac{\partial \psi^{(1)}}{\partial Z} + \frac{V_{\rm p}^3}{\sigma^2 \Omega_{\rm ci}^2} \left[\frac{\partial^3 \psi^{(1)}}{\partial Z \partial X^2} + \frac{\partial^3 \psi^{(1)}}{\partial Z \partial Y^2} \right] = 0, \tag{3.16}$$

$$\frac{\partial \psi^{(1)}}{\partial \tau} + \frac{V_{\rm p}^2}{\sigma} \frac{\partial U_{-{\rm i}z}^{(2)}}{\partial Z} + V_{\rm p} \frac{\partial \psi^{(2)}}{\partial Z} - \frac{\sigma}{V_{\rm p}} \psi^{(1)} \frac{\partial \psi^{(1)}}{\partial Z} = 0, \tag{3.17}$$

$$\frac{\partial \psi^{(1)}}{\partial \tau} - \gamma_{\rm e} V_{\rm p} \frac{\partial N_{\rm e}^{(2)}}{\partial Z} + \gamma_{\rm e} \frac{\partial U_{{\rm e}z}^{(2)}}{\partial Z} + \frac{2V_{\rm p}}{\gamma_{\rm e}} \psi^{(1)} \frac{\partial \psi^{(1)}}{\partial Z} = 0, \tag{3.18}$$

$$\frac{\partial P_{\rm e}^{(2)}}{\partial Z} - \frac{\partial \psi^{(2)}}{\partial Z} - \frac{1}{\gamma_{\rm e}} \psi^{(1)} \frac{\partial \psi^{(1)}}{\partial Z} = 0, \tag{3.19}$$

$$\frac{\partial \psi^{(1)}}{\partial \tau} - V_{\rm p} \frac{\partial P_{\rm e}^{(2)}}{\partial Z} + \gamma_{\rm e} \frac{\partial U_{{\rm e}z}^{(2)}}{\partial Z} + V_{\rm p} \left[1 + \frac{1}{\gamma_{\rm e}} \right] \psi^{(1)} \frac{\partial \psi^{(1)}}{\partial Z} = 0. \tag{3.20}$$

Now, using (3.4)–(3.20), we can readily obtain

$$\frac{\partial \psi^{(1)}}{\partial \tau} + AB \psi^{(1)} \frac{\partial \psi^{(1)}}{\partial Z} + \frac{1}{2} A \frac{\partial}{\partial Z} \left[\frac{\partial^2}{\partial Z^2} + D \left(\frac{\partial^2}{\partial X^2} + \frac{\partial^2}{\partial Y^2} \right) \right] \psi^{(1)} = 0, \tag{3.21}$$

where

$$\begin{aligned} A &= \frac{V_{\rm p}^3}{1 + \mu_- \sigma}, \\ B &= \frac{1}{2} \left[\frac{3}{V_{\rm p}^4} - \frac{\mu (2 - \gamma_{\rm e})}{\gamma_{\rm e}^2} - \frac{3 \mu_- \sigma^2}{V_{\rm p}^4} \right], \\ D &= 1 + \frac{1}{\Omega_{\rm ci}^2} + \frac{\mu_-}{\sigma \Omega_{\rm ci}^2}. \end{aligned} \tag{3.22}$$

The equation (3.21) is known as the Zakharov–Kuznetsov (ZK) equation or the Korteweg–de Vries (KdV) equation in three dimensions.

4. SW solution of the ZK equation

To study the properties of the SWs propagating in a direction making an angle δ with the Z-axis, i.e. with the external magnetic field and lying in the (Z–X) plane, we first rotate the coordinate axes (X, Z) through an angle δ, keeping the Y-axis

https://doi.org/10.1017/S0022377808007733 Published online by Cambridge University Press

fixed. Thus, we transform our independent variables to

$$\zeta = X\cos\delta - Z\sin\delta, \quad \eta = Y, \quad \xi = X\sin\delta + Z\cos\delta, \quad t = \tau. \tag{4.1}$$

This transformation of these independent variables allows us to write the ZK equation in the form

$$\frac{\partial\psi^{(1)}}{\partial t} + \delta_1\psi^{(1)}\frac{\partial\psi^{(1)}}{\partial\xi} + \delta_2\frac{\partial^3\psi^{(1)}}{\partial\xi^3} + \delta_3\psi^{(1)}\frac{\partial\psi^{(1)}}{\partial\zeta} + \delta_4\frac{\partial^3\psi^{(1)}}{\partial\zeta^3} + \delta_5\frac{\partial^3\psi^{(1)}}{\partial\xi^2\partial\zeta}$$
$$+ \delta_6\frac{\partial^3\psi^{(1)}}{\partial\xi\partial\zeta^2} + \delta_7\frac{\partial^3\psi^{(1)}}{\partial\xi\partial\eta^2} + \delta_8\frac{\partial^3\psi^{(1)}}{\partial\zeta\partial\eta^2} = 0, \tag{4.2}$$

where

$$\delta_1 = AB\cos\delta, \quad \delta_2 = \tfrac{1}{2}A(\cos^3\delta + D\sin^2\delta\cos\delta), \quad \delta_3 = -AB\sin\delta,$$
$$\delta_4 = -\tfrac{1}{2}A(\sin^3\delta + D\sin\delta\cos^2\delta),$$
$$\delta_5 = A[D(\sin\delta\cos^2\delta - \tfrac{1}{2}\sin^3\delta) - \tfrac{3}{2}\sin\delta\cos^2\delta], \tag{4.3}$$
$$\delta_6 = -A[D(\sin^2\delta\cos\delta - \tfrac{1}{2}\cos^3\delta) - \tfrac{3}{2}\sin^2\delta\cos\delta],$$
$$\delta_7 = \tfrac{1}{2}AD\cos\delta, \quad \delta_8 = -\tfrac{1}{2}AD\sin\delta.$$

We now look for a steady-state solution of this ZK equation in the form

$$\psi^{(1)} = \psi_0(Z), \tag{4.4}$$

where

$$Z = \xi - u_0\tilde{T}, \quad t = \tilde{T},$$

in which u_0 is a constant speed normalized by the ion-acoustic speed ($C_{\rm i}$). Using this transformation, we get

$$\frac{\partial}{\partial\xi} = \frac{\partial}{\partial Z}, \quad \frac{\partial}{\partial t} = \frac{\partial}{\partial\tilde{T}} - u_0\frac{\partial}{\partial Z}, \quad \frac{\partial}{\partial\zeta} \to 0, \quad \frac{\partial}{\partial\eta} \to 0. \tag{4.5}$$

Therefore, from (4.2), we can write

$$\frac{d\psi_0}{d\tilde{T}} - u_0\frac{d\psi_0}{dZ} + \delta_1\psi_0\frac{d\psi_0}{dZ} + \delta_2\frac{d^3\psi_0}{dZ^3} = 0. \tag{4.6}$$

At stationary state $(d\psi_0/d\tilde{T}) \to 0$. So, we can write the ZK equation in steady-state form as

$$-u_0\frac{d\psi_0}{dZ} + \delta_1\psi_0\frac{d\psi_0}{dZ} + \delta_2\frac{d^3\psi_0}{dZ^3} = 0. \tag{4.7}$$

Now, using the appropriate boundary conditions, viz., $\psi^{(1)} \to 0$, $(d\psi^{(1)}/dZ) \to 0$, $(d^2\psi^{(1)}/dZ^2) \to 0$ as $Z \to \pm\infty$, the SW solution of this equation is given by

$$\psi_0(Z) = \psi_m\,\mathrm{sech}^2(\kappa Z), \tag{4.8}$$

where $\psi_m = 3u_0/\delta_1$ is the amplitude and $\kappa = \sqrt{u_0/4\delta_2}$ is the inverse of the width of the SWs. It is clear from (3.9), (3.22), and (4.3) that as $A > 0$, depending on whether B is positive or negative, the SWs will be associated with either positive potential ($\psi_m > 0$) or negative potential ($\psi_m < 0$). Therefore, there exists SWs associated with positive (negative) potential when $B > 0$ ($B < 0$).

https://doi.org/10.1017/S0022377808007733 Published online by Cambridge University Press

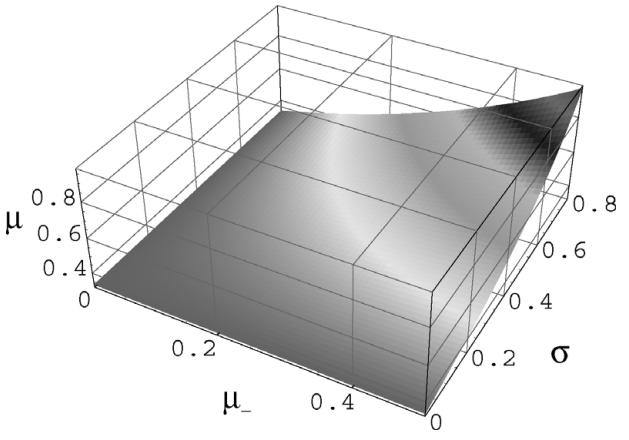

Figure 1. The $B = 0$ surface plot (i.e. the variation of μ with μ_- and σ for $\gamma_e = 1$) above which $\psi_m > 0$ and below which $\psi_m < 0$.

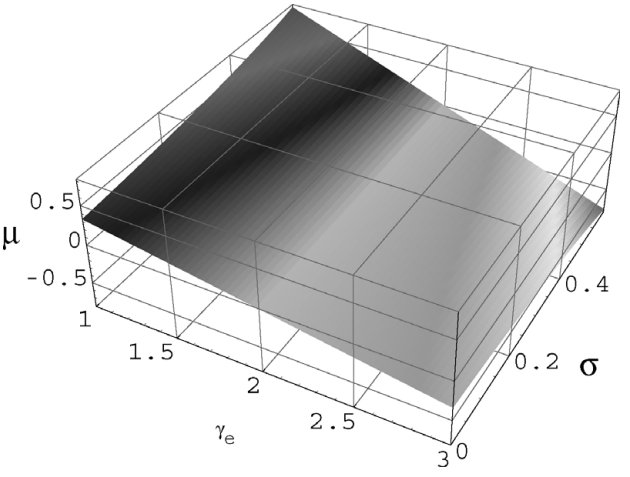

Figure 2. The $B = 0$ surface plot (i.e. the variation of μ with γ_e and σ for $\mu_- = 0.6$) above which $\psi_m > 0$ and below which $\psi_m < 0$.

Figures 1 and 2 represent a $B = 0$ surface plot showing the variation of μ with μ_- and σ (γ_e and σ). This two figures indicate that the upper (lower) region of the surface corresponds to $B > 0$ ($B < 0$), i.e. they correspond to the positive (negative) DIA SWs. Figure 1 shows that the critical value of μ (which is 0.439 for $\mu_- = 0.3$ and $\sigma = 0.4$) increases as the values of both μ_- and σ increase. Figure 2 shows that the critical value of μ (which is 0.214 for $\gamma_e = 1.5$ and $\sigma = 0.2$) decreases as the value of γ_e increases, and the critical value of μ increases (decreases) with the increasing value of σ for a lower (higher) value of γ_e. It is observed from (3.9), (3.22), (4.3), and $\psi_m = 3u_0/\delta_1$ that the amplitude (ψ_m) is a nonlinear function of δ, μ, μ_-, σ, and γ_e. The variations of ψ_m (for positive and negative potentials) with δ, μ, μ_-, σ, and γ_e are shown in Figs 3–8. Figure 3 shows the variation of the amplitude of the positive solitary potential ($\psi_m > 0$) with δ and μ_- for $\mu = 0.7$, $u_0 = 1.0$, $\sigma = 0.2$, and $\gamma_e = 1.0$. This shows that the amplitude increases with increasing

https://doi.org/10.1017/S0022377808007733 Published online by Cambridge University Press

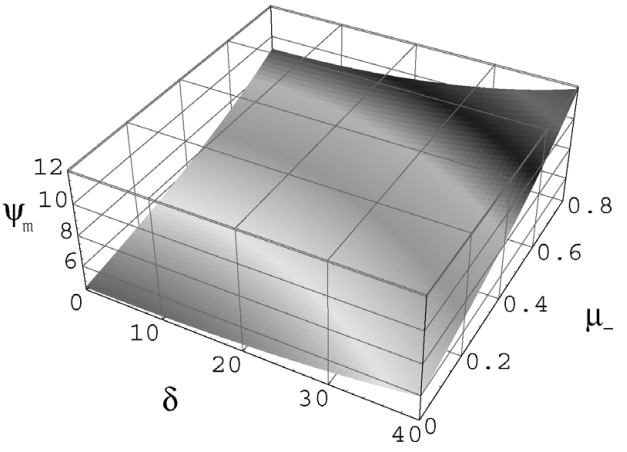

Figure 3. The variation of the amplitude of the positive solitary potential ($\psi_m > 0$) with δ and μ_- for $\mu = 0.7$, $u_0 = 1.0$, $\sigma = 0.2$, and $\gamma_e = 1.0$.

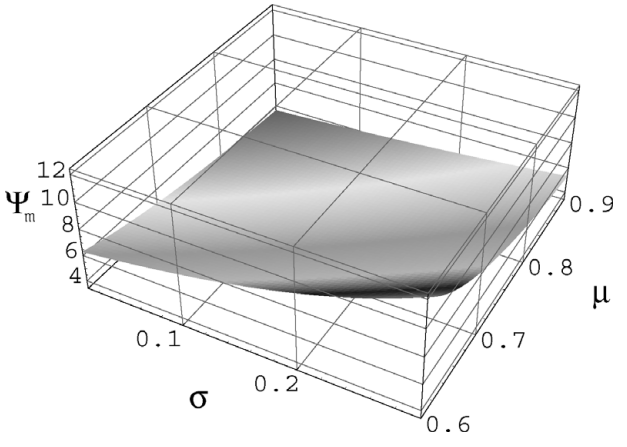

Figure 4. The variation of the amplitude of the positive solitary potential ($\psi_m > 0$) with σ and μ for $\mu_- = 0.4$, $u_0 = 1.0$, $\delta = 20°$, and $\gamma_e = 1.0$.

values of both of δ and μ_-. Figure 4 shows the variation of the amplitude of the positive solitary potential ($\psi_m > 0$) with σ and μ for $\mu_- = 0.4$, $u_0 = 1.0$, $\delta = 20°$, and $\gamma_e = 1.0$. This shows that the amplitude increases (decreases) with increasing values of σ (μ). Figure 5 shows the variation of the amplitude of the positive solitary potential ($\psi_m > 0$) with σ and γ_e for $\mu = 0.9$, $u_0 = 1.0$, $\mu_- = 0.4$, and $\delta = 10°$. This figure indicates that the amplitude decreases as the value of γ_e increases. Figure 6 shows the variation of the amplitude of the negative solitary potential ($\psi_m < 0$) with δ and μ_- for $\sigma = 0.8$, $u_0 = 1.0$, $\mu = 0.2$, and $\gamma_e = 1.0$. This shows that the amplitude increases (decreases) as the value of δ (μ_-) increases. Figure 7 shows the variation of the amplitude of the negative solitary potential ($\psi_m < 0$) with σ and μ for $\mu_- = 0.5$, $u_0 = 1.0$, $\gamma_e = 1.0$, and $\delta = 20°$. This shows that the amplitude increases (decreases) as the value of μ (σ) increases. Figure 8 shows the variation of the amplitude of the negative solitary potential ($\psi_m < 0$) with σ and γ_e for

https://doi.org/10.1017/S0022377808007733 Published online by Cambridge University Press

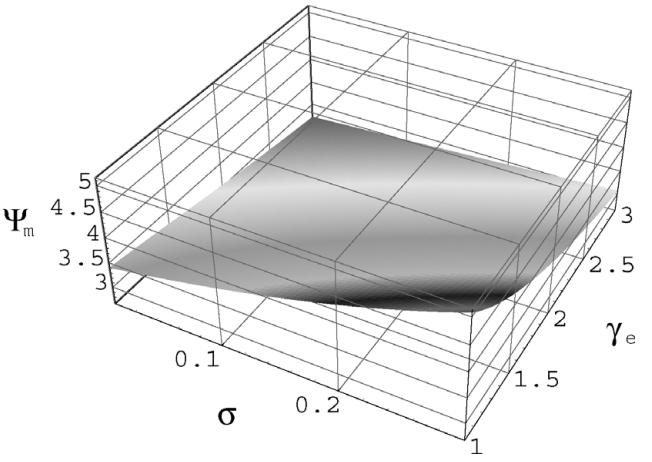

Figure 5. The variation of the amplitude of the positive solitary potential ($\psi_m > 0$) with σ and γ_e for $\mu = 0.9$, $u_0 = 1.0$, $\mu_- = 0.4$, and $\delta = 10^\circ$.

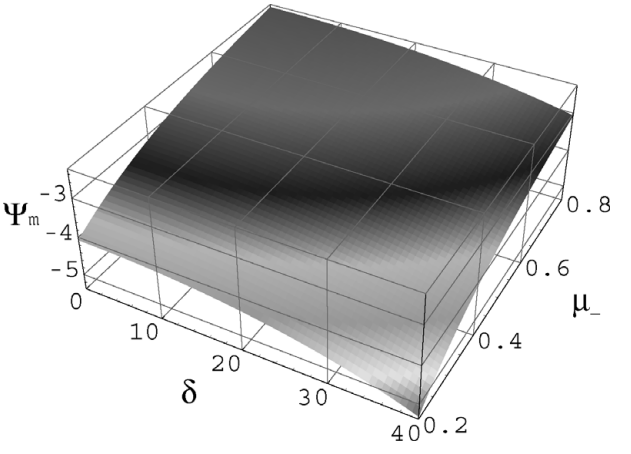

Figure 6. The variation of the amplitude of the negative solitary potential ($\psi_m < 0$) with δ and μ_- for $\sigma = 0.8$, $u_0 = 1.0$, $\mu = 0.2$, and $\gamma_e = 1.0$.

$\mu = 0.01$, $\mu_- = 0.2$, $u_0 = 1.0$, and $\delta = 20^\circ$. This shows that the amplitude increases as the value of γ_e increases.

The magnitude of the external magnetic field has a significant effect only on the width, and not on the amplitude of these SWs. It is found from (3.9), (3.22), (4.3), and $\kappa = \sqrt{u_0/4\delta_2}$ that the width $(1/\kappa)$ is a nonlinear function of Ω_{ci}, δ, σ, μ, μ_-, and γ_e. The variations of the width $(1/\kappa)$ (for positive and negative SWs) with Ω_{ci}, δ, σ, μ, μ_-, and γ_e are represented in Figs 9–11. Figure 9 shows how the width $(1/\kappa)$ changes with δ and Ω_{ci} for $\mu = 0.5$, $u_0 = 1.0$, $\gamma_e = 1.0$, $\mu_- = 0.5$, and $\sigma = 0.4$. This figure shows that the width increases with δ for the lower range, i.e. from 0° to about 50°, but decreases for its higher range, i.e. from about 50° to 90°, and as $\delta \to 90^\circ$, the width goes to 0. This also shows that the width decreases with increasing Ω_{ci}, which is valid for $\delta < 90^\circ$. Figure 10 shows how the width $(1/\kappa)$ changes with γ_e and μ_- for $\Omega_{ci} = 0.2$, $u_0 = 1.0$, $\sigma = 0.2$, $\mu = 0.5$, and $\delta = 20^\circ$. This

https://doi.org/10.1017/S0022377808007733 Published online by Cambridge University Press

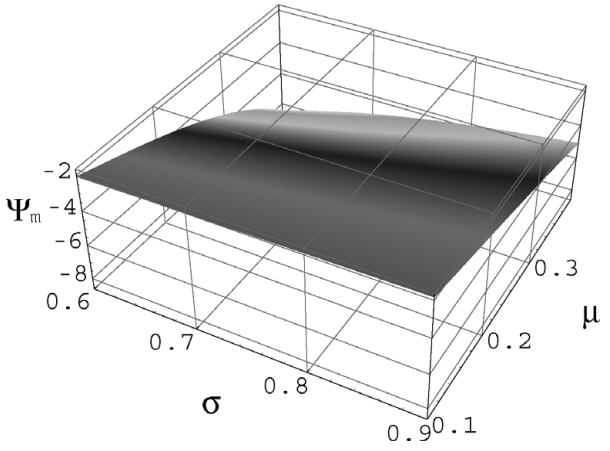

Figure 7. The variation of the amplitude of the negative solitary potential ($\psi_m < 0$) with σ and μ for $\mu_- = 0.5$, $u_0 = 1.0$, $\gamma_e = 1.0$, and $\delta = 20°$.

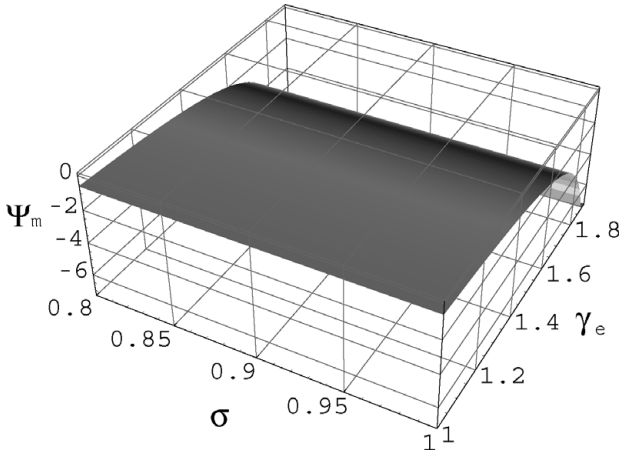

Figure 8. The variation of the amplitude of the negative solitary potential ($\psi_m < 0$) with σ and γ_e for $\mu = 0.01$, $\mu_- = 0.2$, $u_0 = 1.0$, and $\delta = 20°$.

figure indicates that the width increases with increasing values of both γ_e and μ_-. Figure 11 shows how the width $(1/\kappa)$ changes with μ and σ for $\Omega_{ci} = 0.5$, $u_0 = 1.0$, $\gamma_e = 1.0$, $\mu_- = 0.5$, and $\delta = 20°$. This figure indicates that the width decreases with increasing values of both μ and σ.

5. Instability analysis

We now study the instability of the obliquely propagating SW, discussed in the previous section, by the method of small-k perturbation expansion (Rowlands 1969; Infeld 1972, 1985; Infeld and Rowlands 1973; Das and Verheest 1989; Mamun and Cairns 1996). We first assume that

$$\psi^{(1)} = \psi_0(Z) + \phi(Z, \zeta, \eta, t), \tag{5.1}$$

https://doi.org/10.1017/S0022377808007733 Published online by Cambridge University Press

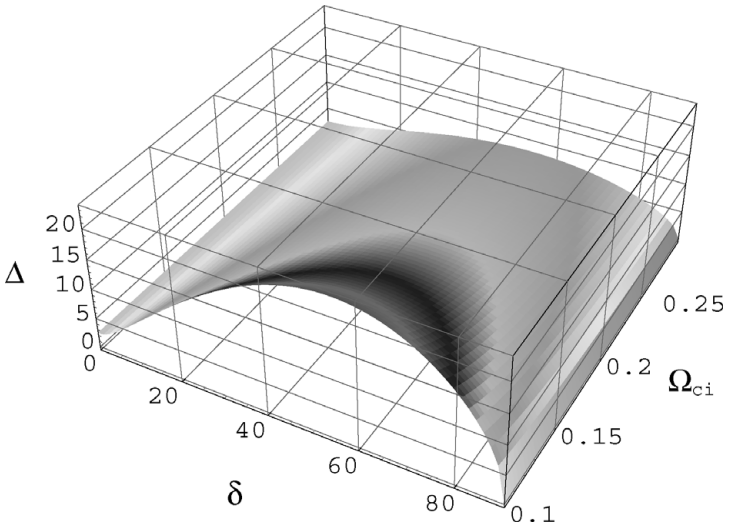

Figure 9. The variation of the width ($\Delta = 1/\kappa$) with δ and Ω_{ci} for $\mu = 0.5$, $u_0 = 1.0$, $\gamma_e = 1.0$, $\mu_- = 0.5$, and $\sigma = 0.4$.

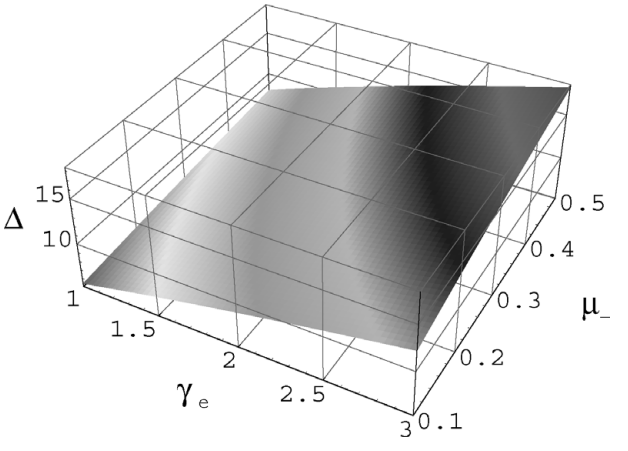

Figure 10. The variation of the width ($\Delta = 1/\kappa$) with γ_e and μ_- for $\Omega_{ci} = 0.2$, $u_0 = 1.0$, $\sigma = 0.2$, $\mu = 0.5$, and $\delta = 20°$.

where ψ_0 is defined by (4.8) and for a long-wavelength plane wave perturbation in a direction with direction cosines, (l_ζ, l_η, l_ξ), ϕ is given by

$$\phi = \varphi(Z) e^{i[k(l_\zeta \zeta + l_\eta \eta + l_\xi Z) - \omega t]}, \tag{5.2}$$

in which $l_\zeta^2 + l_\eta^2 + l_\xi^2 = 1$ and, for small k, $\varphi(Z)$ and ω can be expanded as

$$\varphi(Z) = \varphi_0(Z) + k\varphi_1(Z) + k^2\varphi_2(Z) + \cdots, \tag{5.3}$$

$$\omega = k\omega_1 + k^2\omega_2 + \cdots. \tag{5.4}$$

https://doi.org/10.1017/S0022377808007733 Published online by Cambridge University Press

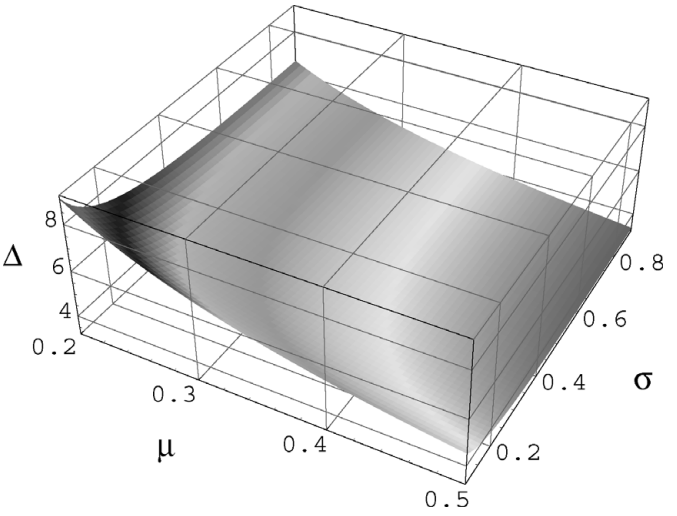

Figure 11. The variation of the width ($\Delta = 1/\kappa$) with μ and σ for $\Omega_{ci} = 0.5$, $u_0 = 1.0$, $\gamma_e = 1.0$, $\mu_- = 0.5$, and $\delta = 20°$.

Now, substituting (5.1) into (4.2) and linearizing with respect to ϕ, we can express the linearized ZK equation in the form

$$\frac{\partial \phi}{\partial t} - u_0 \frac{\partial \phi}{\partial Z} + \delta_1 \psi_0 \frac{\partial \phi}{\partial Z} + \delta_1 \phi \frac{\partial \psi_0}{\partial Z} + \delta_2 \frac{\partial^3 \phi}{\partial Z^3} + \delta_3 \psi_0 \frac{\partial \phi}{\partial \zeta} + \delta_4 \frac{\partial^3 \phi}{\partial \zeta^3} + \delta_5 \frac{\partial^3 \phi}{\partial Z^2 \partial \zeta}$$

$$+ \delta_6 \frac{\partial^3 \phi}{\partial Z \partial \zeta^2} + \delta_7 \frac{\partial^3 \phi}{\partial Z \partial \eta^2} + \delta_8 \frac{\partial^3 \phi}{\partial \zeta \partial \eta^2} = 0. \tag{5.5}$$

Our main object is to find ω_1 by solving the zeroth-, first-, and second-order equations obtained from (5.2)–(5.5). The zeroth-order equation can be written, after integration, as

$$(-u_0 + \delta_1 \psi_0)\varphi_0 + \delta_2 \frac{d^2 \varphi_0}{dZ^2} = C, \tag{5.6}$$

where C is an integration constant. It is clear from (4.7) that the homogeneous part of this equation has two linearly independent solutions, namely

$$f = \frac{d\psi_0}{dZ}, \tag{5.7}$$

$$g = f \int^Z \frac{dZ}{f^2}. \tag{5.8}$$

Therefore, the general solution of this zeroth-order equation can be written as

$$\varphi_0 = C_1 f + C_2 g - C f \int^Z \frac{g}{\delta_2}\, dZ + C g \int^Z \frac{f}{\delta_2}\, dZ, \tag{5.9}$$

where C_1 and C_2 are two integration constants, and δ_2 is defined by (4.3). Now, evaluating all integrals, the general solution of this zeroth-order equation, for φ_0 not tending to $\pm\infty$ as $Z \to \pm\infty$, can finally be simplified to

$$\varphi_0 = C_1 f. \tag{5.10}$$

https://doi.org/10.1017/S0022377808007733 Published online by Cambridge University Press

The first-order equation, i.e., the equation with terms linear in k, obtained from (5.2)–(5.5) and (5.10), can be expressed, after integration, as

$$(-u_0 + \delta_1\psi_0)\varphi_1 + \delta_2 \frac{d^2\varphi_1}{dZ^2} = iC_1(\alpha_1 + \beta_1 \tanh^2 \kappa Z)\psi_0 + K, \tag{5.11}$$

where K is another integration constant, and α_1 and β_1 are given by

$$\begin{aligned} \alpha_1 &= (\omega_1 + l_\xi u_0) - \tfrac{1}{2}\psi_m \mu_1 + 2\kappa^2 \mu_2, \\ \beta_1 &= \tfrac{1}{2}\psi_m \mu_1 - 6\kappa^2 \mu_2, \\ \mu_1 &= \delta_1 l_\xi + \delta_3 l_\zeta, \\ \mu_2 &= 3\delta_2 l_\xi + \delta_5 l_\zeta. \end{aligned} \tag{5.12}$$

Now, following the same procedure, the general solution of this first-order equation, for φ_1 not tending to $\pm\infty$ as $Z \to \pm\infty$, can be written as

$$\varphi_1 = K_1 f + \frac{iC_1}{8\delta_2\kappa^2}\left[(\alpha_1 + \beta_1)Zf + \frac{2}{3}(3\alpha_1 + \beta_1)\psi_0\right]. \tag{5.13}$$

The second-order equation, i.e. the equation with terms involving k^2, obtained from (5.5) after substituting (5.2)–(5.4), can be written as

$$\left[-u_0\frac{d}{dZ} + \delta_1\frac{d}{dZ}\psi_0 + \delta_2\frac{d^3}{dZ^3}\right]\varphi_2 = i\omega_2\varphi_0 + i(\omega_1 + l_\xi u_0)\varphi_1 - i\mu_1\psi_0\varphi_1 + \mu_3\frac{d\varphi_0}{dZ} - i\mu_2\frac{d^2\varphi_1}{dZ^2}, \tag{5.14}$$

where

$$\mu_3 = 3\delta_2 l_\xi^2 + 2\delta_5 l_\zeta l_\xi + \delta_6 l_\zeta^2 + \delta_7 l_\eta^2. \tag{5.15}$$

The solution of this second-order equation exists if the right-hand side is orthogonal to a kernel of the operator adjoint to the operator

$$-u_0\frac{d}{dZ} + \delta_1\frac{d}{dZ}\psi_0 + \delta_2\frac{d^3}{dZ^3}. \tag{5.16}$$

This kernel, which must tend to zero as $Z \to \pm\infty$, is $(\psi_0/\psi_m) = \operatorname{sech}^2(\kappa Z)$. Thus we can write the following equation determining ω_1:

$$\int_{-\infty}^{\infty} \psi_0\left[i\omega_2\varphi_0 + i(\omega_1 + l_\xi u_0)\varphi_1 - i\mu_1\psi_0\varphi_1 + \mu_3\frac{d\varphi_0}{dZ} - i\mu_2\frac{d^2\varphi_1}{dZ^2}\right]dZ = 0. \tag{5.17}$$

Now, substituting the expressions for φ_0 and φ_1 given by (5.10) and (5.13), respectively, and then performing the integration, we arrive at the following dispersion relation:

$$\omega_1 = \Omega - l_\xi u_0 + (\Omega^2 - \Upsilon)^{1/2}, \tag{5.18}$$

where

$$\Omega = \tfrac{2}{3}(\psi_m \mu_1 - 2\mu_2\kappa^2), \tag{5.19}$$

$$\Upsilon = \tfrac{16}{45}(\psi_m^2\mu_1^2 - 3\psi_m\mu_1\mu_2\kappa^2 - 3\mu_2^2\kappa^4 + 12\delta_2\mu_3\kappa^4). \tag{5.20}$$

It is clear from the dispersion relation (5.18) that there is always instability if $(\Upsilon - \Omega^2) > 0$. Thus, using (3.22), (4.3), (5.12), (5.15), (5.19), and (5.20), we can

https://doi.org/10.1017/S0022377808007733 Published online by Cambridge University Press

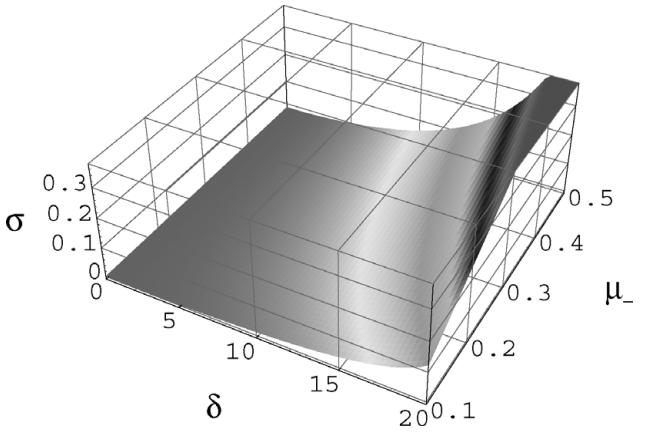

Figure 12. The $S_i = 0$ surface plot (i.e. the variation of σ with δ and μ_- for $\Omega_{ci} = 0.5$, $l_\zeta = 0.6$, and $l_\eta = 0.4$) above which the SWs become unstable and below which the SWs become stable.

express the instability criterion as

$$S_i > 0, \tag{5.21}$$

with

$$S_i = l_\eta^2[\Omega_{ci}^2 + Y\sin^2\delta] + l_\zeta^2[\Omega_{ci}^2 - \tfrac{5}{3}(Y + \Omega_{ci}^2)\tan^2\delta], \tag{5.22}$$

$$Y = \frac{\sigma + \mu_-}{\sigma}. \tag{5.23}$$

It has been observed that the γ_e and μ values have no any effect on whether the SWs become stable or unstable. We have graphically obtained the parametric regimes (values of σ, δ, μ_-, Ω_{ci}, l_ζ, and l_η) for which the SWs become stable and unstable. These are shown in Figs 12 and 13, which indicate that for the parameters above (below) the surface the SWs become unstable (stable). Figure 12 represents $S_i = 0$ surface plot showing the variation of σ with δ and μ_- for $\Omega_{ci} = 0.5$, $l_\zeta = 0.6$, and $l_\eta = 0.4$. This indicates that, as the values of δ and μ_- increase, the value of σ for which the SWs become unstable increases. Figure 13 represents the $S_i = 0$ surface plot showing the variation of Ω_{ci} with l_ζ and l_η for $\sigma = 0.5$, $\mu_- = 0.5$, and $\delta = 10^\circ$. This figure indicates that as the value of l_ζ (l_η) increases, the value of Ω_{ci} for which the SWs become unstable increases (decreases).

If this instability criterion $S_i > 0$ is satisfied, the growth rate $\Gamma = (\Upsilon - \Omega^2)^{1/2}$ of the unstable perturbation of these SWs is given by

$$\Gamma = \frac{2}{15^{1/2}} \frac{u_0[(Y + \Omega_{ci}^2)S_i]^{1/2}}{\Omega_{ci}^2 + Y\sin^2\delta}. \tag{5.24}$$

Equation (5.24), together with (5.22) and (5.23), clearly indicate that the growth rate Γ of the unstable perturbation is a linear function of u_0, but a nonlinear function of δ, Ω_{ci}, σ, μ_-, l_ζ, and l_η. The nonlinear variations of Γ with δ, Ω_{ci}, σ, μ_-, l_ζ, and l_η are shown in Figs 14–16. Figure 14 shows how the value of Γ changes with σ and μ_- for $u_0 = 1.0$, $\Omega_{ci} = 0.5$, $\delta = 5^\circ$, $l_\zeta = 0.5$, and $l_\eta = 0.5$. This figure indicates that, as the value of μ_- (σ) increases, the value of the growth rate Γ of the unstable perturbation increases (decreases). Figure 15 shows how the

https://doi.org/10.1017/S0022377808007733 Published online by Cambridge University Press

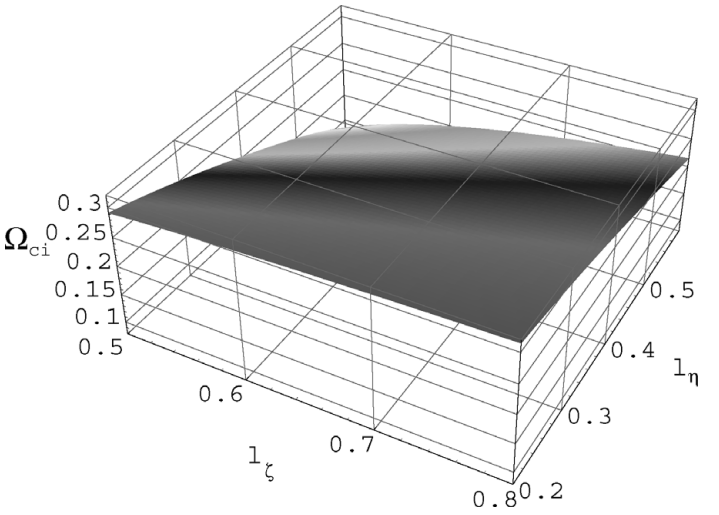

Figure 13. The $S_i = 0$ surface plot (i.e. the variation of Ω_{ci} with l_ζ and l_η for $\sigma = 0.5$, $\mu_- = 0.5$, and $\delta = 10°$) above which the SWs become unstable and below which the SWs become stable.

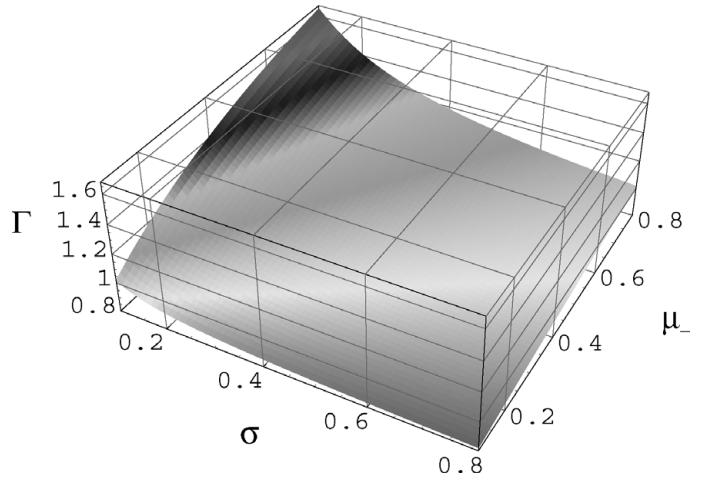

Figure 14. The variation of Γ with σ and μ_- for $u_0 = 1.0$, $\Omega_{ci} = 0.5$, $\delta = 5°$, $l_\zeta = 0.5$, and $l_\eta = 0.5$.

value of Γ changes with δ and Ω_{ci} for $u_0 = 1.0$, $\sigma = 0.6$, $\mu_- = 0.2$, $l_\zeta = 0.4$, and $l_\eta = 0.4$. This figure indicates that the growth rate Γ of the unstable perturbation decreases with increasing values of both δ and Ω_{ci}. Figure 16 shows how the value of Γ changes with l_η and l_ζ for $u_0 = 1.0$, $\delta = 5°$, $\sigma = 0.5$, $\Omega_{ci} = 0.5$ and $\mu_- = 0.1$. This shows that the value of Γ increases with increasing values of both l_η and l_ζ.

6. Discussion

We have considered a fully ionized collisionless magneto dusty plasma consisting of cold positive and negative ions, hot adiabatic inertia-less electrons, and negatively

https://doi.org/10.1017/S0022377808007733 Published online by Cambridge University Press

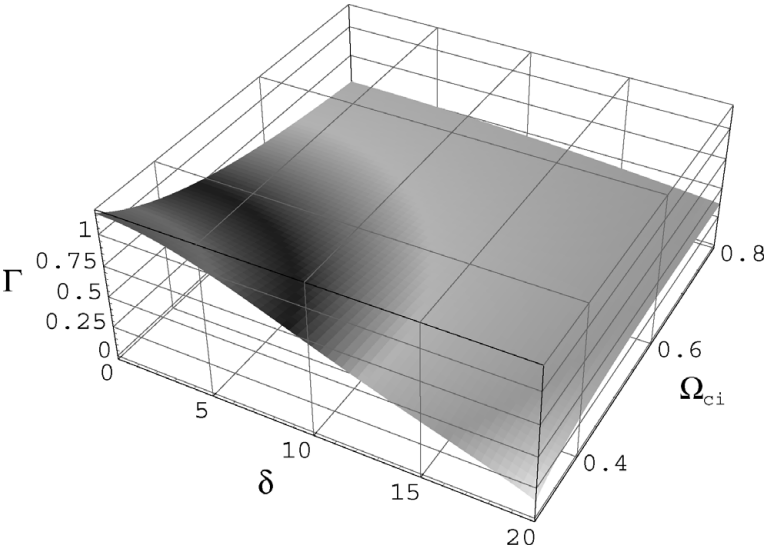

Figure 15. The variation of Γ with δ and Ω_{ci} for $u_0 = 1.0$, $\sigma = 0.6$, $\mu_- = 0.2$, $l_\zeta = 0.4$, and $l_\eta = 0.4$.

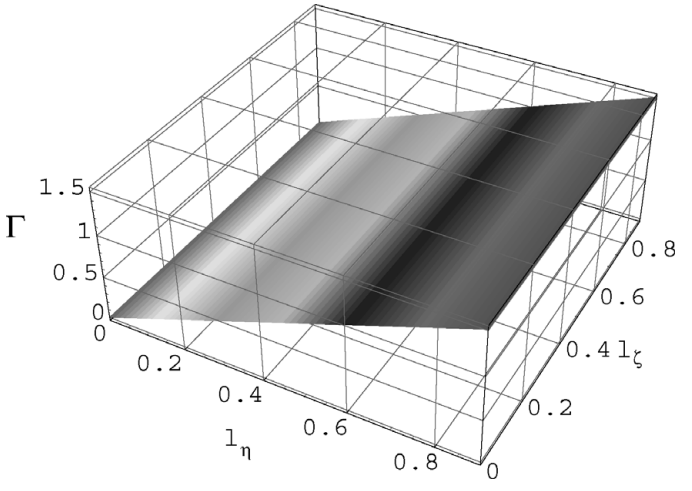

Figure 16. The variation of Γ with l_η and l_ζ for $u_0 = 1.0$, $\delta = 5°$, $\sigma = 0.5$, $\Omega_{ci} = 0.5$ and $\mu_- = 0.1$.

charged static dust, and have studied the DIA SWs associated with both positive and negative potentials by deriving the ZK equation. We have then analyzed their multi-dimensional instability by the small-k perturbation expansion method. The results that have been obtained from this investigation can be summarized as follows.

(a) The SWs may be associated with either positive or negative potential, depending on the values of μ, μ_-, σ, and γ_e.

https://doi.org/10.1017/S0022377808007733 Published online by Cambridge University Press

(b) The amplitude of the positive SWs increases with increasing values of μ_-, σ, and δ, but decreases with increasing μ and γ_e.

(c) The amplitude of the negative SWs increases with increasing values of μ, δ, and γ_e, but decreases with increasing μ_- and σ.

(d) The width of the SWs (both for positive and negative potentials) increases for the lower range of δ (from 0° to about 50°), but decreases for its higher range (from 50° to about 90°).

(e) The width of the SWs for both positive and negative potentials increases with increasing values of γ_e and μ_-, but decreases with increasing values of μ and σ.

(f) The magnitude of the external magnetic field $\mathbf{B}_0$ has no direct effect on the SW amplitude. However, it does have a direct effect on the width of the SWs, and we have found that, as the magnitude of $\mathbf{B}_0$ increases, the width of the waves decreases, i.e. the magnetic field makes the solitary structures more spiky.

(g) The μ and γ_e values have no effect on either whether the SWs will be stable or unstable nor on the growth rate of Γ of the unstable perturbation.

(h) The value of σ for which the SWs become unstable increases with increasing values of δ and μ_-, with the other parameters constant.

(i) The value of Ω_{ci} for which the SWs become unstable increases with increasing values of l_ζ, but decreases with increasing values of l_η, with the other parameters constant.

(j) The growth rate Γ of the unstable perturbation decreases with increasing values of σ and δ, but increases with increasing values of μ_-, with the other parameters constant.

(k) The value of Γ decreases for the lower range of δ (from 0° to about 10°), and increases for the higher range of δ with the increasing magnitude of the magnetic field.

(l) The growth rate Γ increases with increasing values of both l_η and l_ζ.

As $\delta \to 90°$, the width goes to 0, and the amplitude goes to ∞. It is likely that for large angles the assumption that the waves are electrostatic is no longer valid, and we should look for fully electromagnetic structures.

The ranges ($\sigma = 0 - 0.9$, $\mu = 0 - 0.9$, and $\mu_- = 0 - 0.8$) of the dusty plasma parameters used in this numerical analysis are very wide. Therefore, the dusty plasma parameters (viz. σ, μ, and μ_-) corresponding to space (Horanyi and Mendis 1985, 1986; Geortz 1989; Mendis and Horanyi 1991; Montmerle 1991; Northrop 1992; Ciolek and Mouschovias 1993; Mendis and Rosenberg 1994; Nakano et al. 1996; Shukla and Mamun 2002) and laboratory dusty plasmas (Pieper and Goree 1996; Shukla et al. 1997; Nakamura et al. 1999) are certainly within these ranges (viz. $\sigma = 0{-}0.9$, $\mu = 0{-}0.9$, and $\mu_- = 0{-}0.8$). Therefore, our present results may be useful for understanding the localized electrostatic disturbance in space (Horanyi and Mendis 1985, 1986; Geortz 1989; Mendis and Horanyi 1991; Montmerle 1991; Northrop 1992; Ciolek and Mouschovias 1993; Mendis and Rosenberg 1994; Nakano et al. 1996; Shukla and Mamun 2002) and laboratory (Pieper and Goree 1996; Shukla et al. 1997; Nakamura et al. 1999) dusty plasmas.

https://doi.org/10.1017/S0022377808007733 Published online by Cambridge University Press

It may be mentioned here that we have used a reductive perturbation method and a small-k perturbation expansion that are valid for small but finite-amplitude SWs and long-wavelength perturbation modes. Since in many astrophysical situations there are extremely large-amplitude SWs and short-wavelength perturbation modes, we propose to develop a more exact theory for instability analysis of arbitrary-amplitude SWs and arbitrary-wavelength perturbation modes, through a generalization of our present work to such waves and modes.

Acknowledgements

One of the authors (MGMA) acknowledges the financial support of National University (Bangladesh) and the Ministry of Education (Bangladesh) for granting his deputation during the course of this research work.

References

Barkan, A., D'Angelo, N. and Merlino, R. L. 1996 *Planet. Space Sci.* **44**, 239.

Bharuthram, R. and Shukla, P. K. 1992 *Planet. Space Sci.* **40**, 973.

Birk, G. T., Copp, A. and Shukla, P. K. 1996 *Phys. Plasmas* **3**, 3564.

Copp, A., Birk, G. T. and Shukla, P. K. 1997 *Phys. Plasmas* **4**, 4414.

Ciolek, G. E. and Mouschovias, T. Ch. 1993 *Astrophys. J.* **418**, 774.

Das, P. K. and Verheest, F. 1989 *J. Plasma Phys.* **41**, 171.

El-Labany, S. K. and El-Shamy, E. F. 2004 *Astrophys. Space Sci.* **293**, 295.

Geortz, C. K. 1989 *Rev. Geophys.* **27**, 271.

Horanyi, M. and Mendis, D. A. 1985 *Astrophys. J.* **294**, 357.

Horanyi, M. and Mendis, D. A. 1986 *Astrophys. J.* **307**, 800.

Infeld, E. 1972 *J. Plasma Phys.* **8**, 105.

Infeld, E. 1985 *J. Plasma Phys.* **33**, 171.

Infeld, E. and Rowlands, G. 1973 *J. Plasma Phys.* **10**, 293.

Kourakis, I., Shukla, P. K. and Morfill, G. E. 2005 *New J. Phys.* **7**, 153.

Laedke, E. W. and Spatschek, K. H. 1982 *J. Plasma Phys.* **28**, 469.

Lee, L. C. and Kan, J. R. 1981 *Phys. Fluids* **24**, 430.

Mamun, A. A. 2008 *Phys. Lett.* A **372**, 1490.

Mamun, A. A. and Cairns, R. A. 1996 *J. Plasma Phys.* **56**, 175.

Mamun, A. A. and Shukla, P. K. 2002a *IEEE Trans. Plasma Sci.* **30**, 720.

Mamun, A. A. and Shukla, P. K. 2002b *Phys. Plasmas* **9**, 1468.

Mamun, A. A. and Shukla, P. K. 2005 *Plasma Phys. Control. Fusion* **47**, A1.

Mendis, D. A. and Horanyi, M. 1991 In: *Cometary Plasma Processes (AGU Monograph, 61)*. Washington, D.C.: American Geophysical Union, p. 17.

Mendis, D. A. and Rosenberg, M. 1994 *Annu. Rev. Astron. Astrophys.* **32**, 419.

Merlino, R. L. and Goree, J. 2004 *Phys. Today* **57**, 32.

Montmerle, T. 1991 In: *The Physics of Star Formation and Early Stellar Evolution* (ed. C. J. Lada and N. D. Kylafis). Dordrecht: Kluwer, p. 675.

Nakamura, Y., Bailung, H. and Shukla, P. K. 1999 *Phys. Rev. Lett.* **83**, 1602.

Nakamura, Y. and Sharma, A. 2001 *Phys. Plasmas* **8**, 3921.

Nakano, T., Nishi, R. and Umebayashi, T. 1996 In: *The Role of Dust in the Formation of Stars* (ed. H. U. Käufle and R. Siebenmorgen). Berlin: Springer, p. 675.

Northrop, T. G. 1992 *Phys. Scripta* **45**, 475.

Pieper, J. B. and Goree, J. 1996 *Phys. Rev. Lett.* **77**, 3137.

Rahman, A., Sayed, F. and Mamun, A. A. 2007 *Phys. Plasmas* **14**, 034503.

Rowlands, G. 1969 *J. Plasma Phys.* **3**, 567.

Rosenberg, M. and Merlino, R. L. 2007 *Planet. Space Sci.* **55**, 1464.

Rosenberg, M. and Shukla, P. K. 2002 *J. Geophys. Res.* **107**, SIA 21-1.

Sayed, F., Haider, M. M., Mamun, A. A., Shukla, P. K., Eliasson, B. and Adhikary, N. 2008 *Phys. Plasmas* **15**, 063701.

Shukla, P. K., Amin, M. R. and Morfill, G. E. 1999 *Phys. Scripta* **59**, 389.

Shukla, P. K., Birk, G. T. and Morfill, G. E. 1997 *Phys. Scripta* **56**, 299.

Shukla, P. K. and Mamun, A. A. 2002 *Introduction to Dusty Plasma Physics*. Bristol: IOP Publishing Ltd.

Shukla, P. K. and Mamun, A. A. 2003 *New J. Phys.* **5**, 17.1.

Shukla, P. K. and Rosenberg, M. 1999 *Phys. Plasmas* **6**, 1038.

Shukla, P. K. and Silin, V. P. 1992 *Phys. Scripta* **45**, 508.

Shukla, P. K. and Yu, M. Y. 1978 *J. Math. Phys.* **19**, 2506.

Verheest, F. 2000 *Waves in Dusty Plasmas*. Dordrecht: Kluwer Academic.

Vranjes, J., Pandey, B. P. and Poedts, S. 2005 *Planet. Space Sci.* **54**, 695.

Witt, E. and Lotko, W. 1983 *Phys. Fluids* **26**, 2176.